International Journal for Multidisciplinary Research (IJFMR)
E-ISSN: 2582-2160 ● Website: www.ijfmr.com ● Email: editor@ijfmr.com

Magnetization Dynamics Along A Magnetic Nanowire Under A Localized Thermal Gradient

Ferdouse Yesmin

Lecturer in Physics, Department of Electrical and Electronic Engineering, North Western University, Khulna, Bangladesh

Abstract

The magnetization dynamics along a magnetic nanowire under a localized thermal gradient is investigated using the framework of the stochastic Landau-Lifshitz-Gilbert equation. Thermally induced Domain Wall displacement is compared in various cases. The laser width can affect the displacement of the DW inside a nanowire, which is shown here. Also, the distance between DW and laser width can influence DW movement which is compared in this study. These findings highlight the importance of optimizing thermal gradient parameters (e.g. spatial extent and proximity to the DW) for reliable control of DW motion in spintronics applications. The study also provides insights into the design of low-energy, thermally driven nanodevices, such as racetrack memories or logic gates, where precise DW manipulation is critical. Future work could explore temperature- dependent material properties, alternative nanostructures, and experimental validation to bridge theoretical predictions with practical implementations.

Keywords: Magnetization Dynamics; Domain Wall Dynamics; Thermal Gradient; sLLG equation.

1. Introduction

Magnetization dynamics has feasible application in data storage technology [1] and logic gates [2]. Magnetization of magnetic nanoparticles must be manipulated in order to be exploited several driving factors are used to control magnetization dynamics in this scenario. A microwave field of constant frequency or variable frequency [3] and spin- polarized electric current [4–7] or spin orbit torque [8–11] are utilized to produce fast magnetization dynamics with minimum energy along a magnetic nanowire to regulate magnetization dynamics. Reversing the magnetization of a single nanoparticle domain and driving the magnetic domain wall (DW) in a magnetic nanowire are two aspects of controlling magnetization dynamics. Magnetic fields [3], spin-polarized currents [4–7], and thermal gradients are examples of conventional driving factors that can affect DWs in magnetic nanostructures. All driving factors, on the other hand, have certain limitations. The energy dissipation rate is proportional to the DW speed when the DW is driven by a magnetic field [12, 13]. In addition, rather than driving a sequence of DWs synchronously, the magnetic field prefers to eliminate undesirable domains and Dws [14–16]. When a spin polarized electric current [5, 17–19] is used to induce DW motion, the DW travels by angular momentum transfer, pushing several

DWs in the same direction. However, in order to achieve a relevant DW speed, the electrical current density must be large, resulting in a joule heating issue [16, 20, 21]. To overcome these issues, the use of a thermal gradient as a DW control parameter has been proposed [9, 22–24]. Thermal gradient can induce fast DW motion while consuming low energy. The thermal gradient may be employed in both magnetic metals (conductors and semiconductors) [25–27] and magnetic insulators [28], unlike an electric current, which is exclusively relevant to metallic systems. Furthermore, the thermal gradient-generated spin current might be a potential way to harvest the heat that has been dissipated in electric circuits [29, 30].

We know according to theoretical perspective, the TG-driven DW dynamics has two theories from different origin. According to macroscopic thermodynamic theories [31, 32] to reduce the system's free energy, a TG provides an entropy torque (ET) that constantly pushes the DW towards the hotter region. On the other hand, according to the microscopic theories [9, 10, 22, 23, 33], to form a magnonic spin current magnons produced in the hotter region diffuse to the colder region. The magnonic spin current exerts torques on the DW while crossing the DW by transferring spin angular momentum. As a result, magnons cause the DW to propagate in the opposite direction of the magnon current [9, 22, 24], toward the hotter region of the nanowire. Also, recent studies demonstrate that the DW can also propagate towards the cold part depending on magnons' behavior [10]. If magnons are transmitted through the DW, then angular momentum transfer leads to DW motion towards the hot part (opposite the direction of magnon propagation), as predicted from Refs. [9, 22, 34]. On the other hand, if magnons are reflected, linear momentum transfer leads to DW motion towards the cold part (the same direction as magnon propagation), as shown in Refs. [8, 33, 35].

This study, inside a permalloy nanowire as shown in Figure 1 using the stochastic-LLG framework observed that the thermal gradient can drive the DW toward the hotter region for different cases. Therefore, this investigation focuses on exploring the physical reason why and under what conditions TG can drive the DW toward the hot region. The conclusions are based on micromagnetic simulations. This paper is structured as follows. Sect. 2 Analytical model and method. Sect. 3 Observations. Sect. 4 Conclusions.

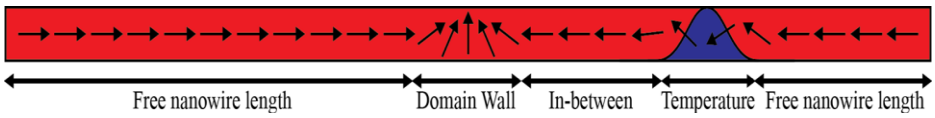

Figure 1. Schematic diagram of a nanowire with a head-to-head DW placed at the center under a localized Gaussian temperature gradient.

2. Analytical Model and Method

In this study, the dynamics of a head-to-head transverse DW (TDW) placed at the center along the x-axis (easy axis) in a Permalloy nanowire of length $L_x = 4.096\ \mu$m and cross-sectional area $S = L_y \times L_z = 32 \times 6\ \text{nm}^2$. The DW width Δ is larger than the dimension of L_y, L_z but much smaller than L_x. A localized thermal gradient (Gaussian shape) as a driving force is applied along the nanowire. The applied highest temperature is far below the Curie temperature T_c. The magnetization dynamics is governed by the stochastic Landau-Lifshitz-Gilbert (sLLG) equation [36–38],

$$\frac{dm}{dt} = -\gamma \mathrm{m} \times (\mathrm{h_{eff}} + \mathrm{h_{th}}) + \alpha \mathrm{m} \times \frac{\partial m}{\partial t} \qquad (1)$$

where, m = M/M_s and M_s are respectively the magnetization direction and the saturation magnetization. α is the Gilbert damping constant and t is measured in the units of $(|\gamma|M_s)^{-1}$ in which γ is the gyromagnetic ratio.

$h_{eff} = \frac{2A}{M_s}\sum_\sigma \frac{\partial m}{\partial x_\sigma} + K_\parallel m_x \hat{x} + h_{dipole}$ is the effective field measured in the units of M_s, where A is the exchange constant, x_σ (σ = 1,2,3) denote Cartesian coordinates x, y, z, $K_\parallel$ is the easy-axis anisotropy, and h_{dipole} is the dipolar field. h_{th} is the thermal stochastic field.

The stochastic LLG equation is solved numerically by MUMAX3 package [38] in which adaptive Heun solver is used. The time step is chosen 10^{-14}s for the cell size $(2 \times 4 \times 6)$ nm^3 and 10^{-15} s for unit cells smaller than $(2 \times 4 \times 6)$ nm^3. The saturation magnetization $M_s = 8 \times 10^5$ A/m and exchange constant $A = 13 \times 10^{-12}$ J/m are used to mimic permalloy in this simulations. It is assumed that the saturation magnetization and exchange constant are temperature-independent. The thermal field follows the Gaussian process characterized by the following statistics

$\langle h_{th,ip}(t) \rangle = 0,$

$\langle h_{th,ip}(t) h_{th,iq}(t+\Delta t) \rangle = \frac{2k_B T_i \alpha_i}{\gamma M_s a^3} \delta_{ij}\, \delta_{pq}\, \delta(\Delta t),$ (2)

where, i and j denote the micromagnetic cells, and p, q represent the Cartesian components of the thermal field. T_i and α_i are respectively the temperature and the Gilbert damping at cell i, and a is the cell size. k_B is the Boltzmann constant [36]. The numerical results presented in this study are averaged over 15 random configurations (for DW velocity).

The Gaussian temperature profile is given by,

$T(x) = T_0 + T_L \exp\left[-\frac{(x-X_L)^2}{2\sigma_L^2}\right]$ (3)

where, $T_0 = 0$ and T_L is the laser temperature. X_L is the laser spot position, and σ_L is the laser width. The temperature gradient profile is given by,

$\nabla_x T(x) = \frac{dT(x)}{dx} = -T_L \frac{(x-X_L)}{\sigma_L^2} \exp\left[-\frac{(x-X_L)^2}{2\sigma_L^2}\right]$ (4)

3. Numerical Results

3.1 DW displacement as a function of laser width

Figure 2 illustrates the impact of varying laser widths on Domain Wall (DW) displacement in a magnetic nanowire under a localized thermal gradient, modeled via the stochastic Landau-Lifshitz-Gilbert (LLG) equation. In this study, total length of the nanowire is 4096nm and total length is devided into 256 regions. Each region is 16nm. In the first case, temperature pick is given at 3064nm which is in 192 region. Temperature is given in total 5 regions by keeping 192 region in the middle. So, the length of laser width is 80nm in this case. The position of DW is in 2648nm. The closest region of the DW from the edge of the laser width is 190. Here, the in between distance from the DW to the laser width is 416nm and in between distance from the DW to the edge of the laser width is 392nm.

In the second case, temperature pick is given at 3192nm which is in 200 region. Temperature is given in total 21 regions by keeping 200 region in the middle. So, the length of laser width is 336nm in this case. The position of DW is in 2648nm. The closest region of the DW from the edge of the laser width is 190. Here, the in between distance from the DW to the laser width is 544nm and in between

distance from the DW to the edge of the laser width is 392nm which is same as the first case. This figure shows that the DW displacement is high when temperature pick at 200 region; for the second case when the length of laser width is higher than the first case. So, we can conclude that DW displacement increases with the increasing laser width. Because, wider lasers create extended thermal gradients, generating stronger entropic forces that drive DW displacement.

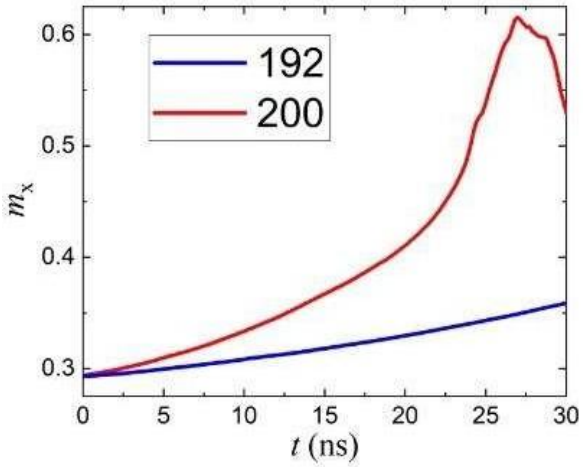

Figure 2. DW displacement as a function of Laser width.

3.2 Fixed DW and Varying Laser Point

Figure 3 highlights the displacement of the DW as a function of the distance between the distance of the DW and the laser point (d). The DW is placed in the middle of the nanowire, which is at DW=2048nm. The temperature is given in various regions, respectively, 253, 228, 203, 178, 153 and 128. So, the in between distances become respectively d=1992nm, 1592nm, 1192nm, 792nm, 392nm and -8nm. From this figure 3 we can see that as the in-between distance (d) decreases (from 1992 nm to 392 nm), the DW displacement increases. This trend aligns with thermally driven DW motion mechanisms. A thermal gradient generates a magnonic spin current or a thermomagnetic force, propelling the DW toward the hotter region (higher temperature). The closer the DW is to the heat source, the steeper the thermal gradient, enhancing the driving force. This behavior is consistent with studies on spin-transfer torques induced by thermal gradients [39]. But when DW reaches very close to the laser point, for d=-8nm (DW very near or past the laser point) we see a random DW motion. This results from two factors. The first is thermal agitation: Near the laser, elevated temperatures amplify thermal fluctuations, which dominate over deterministic forces. The stochastic term in the sLLG equation becomes significant, leading to unpredictable DW dynamics. The second factor is the Gradient Instability: The negative d suggests that the DW has overshot the laser location, potentially encountering a reversed or unstable thermal profile, further disrupting coherent motion.

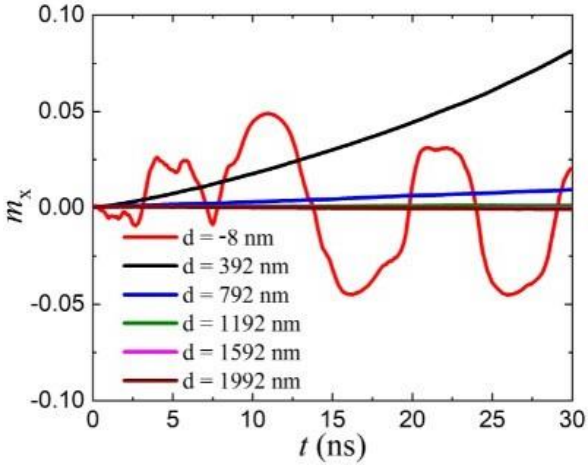

Figure 3. Fixed DW and varying laser point.

3.3 Fixed laser point and moving DW closer to laser point

Figure 4 highlights the DW displacement as a function of in between distance (d) of DW and laser point. Now the laser point is placed at the region 240 which is at 3832nm. The DW is placed in the various regions, respectively, 128, 153, 178, 203, 228 and 253. So that the in between distances become respectively d=1784nm, 1384nm, 984nm, 584nm, 184nm and -216nm. This figure 4 shows DW displacement increased very slowly with decreased in between distance(d). So that we can say, DW moves towards the hot region as the in between distance decreases. This aligns with the thermomagnetic effect, where the thermal gradient drives DW motion toward the hotter region (laser spot) due to entropy-driven forces. For d=184nm and d=-216nm, the DW exhibits random motion. This stochastic behavior arises from enhanced thermal fluctuations near the laser, as modeled by the sLLG equation. At close proximity, the temperature gradient becomes extremely steep, destabilizing the DW dynamics and amplifying the effects of thermal noise.

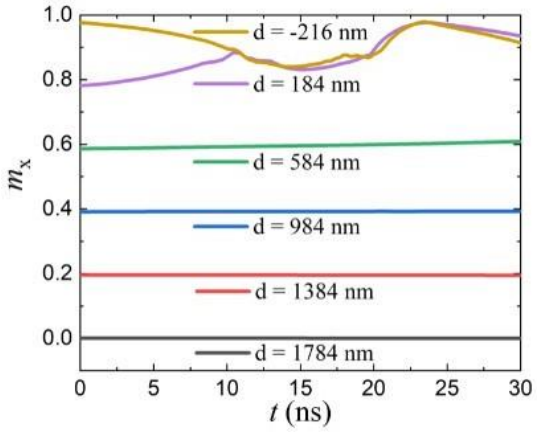

Figure 4. Fixed laser point and varying DW.

4. Conclusions

This study investigated the magnetization dynamics of a transverse domain wall (DW) in a Permalloy nanowire under a localized thermal gradient using micromagnetic simulations based on the stochastic Landau-Lifshitz-Gilbert (sLLG) equation. The displacement of the DW increases with the width of the applied thermal gradient (laser spot). Wider laser profiles generate extended thermal gradients, enhancing

the entropy-driven forces that propel the DW toward the hotter region. The DW displacement is highly sensitive to its initial distance from the laser spot. As the DW approaches the thermal gradient, its motion accelerates due to the steepening thermal gradient. However, when the DW is extremely close to or overlaps with the laser spot, thermal agitation dominates, leading to stochastic behavior and loss of directional coherence. The results align with macroscopic thermodynamic theories, where the DW migrates toward the hotter region to minimize free energy. This supports the role of entropy torque as a driving mechanism under moderate thermal gradients. At elevated temperatures near the laser spot, microscopic magnonic effects and thermal noise become significant, consistent with stochastic LLG dynamics.

References

1. S. S. Parkin, M. Hayashi, and L. Thomas, Science **320**, 190 (2008).
2. D. A. Allwood, G. Xiong, C. Faulkner, D. Atkinson, D. Petit, and R. Cowburn, science **309**, 1688 (2005).
3. N. L. Schryer and L. R. Walker, Journal of Applied Physics **45**, 5406 (1974).
4. L. Berger, Journal of Applied Physics **55**, 1954 (1984).
5. J. C. Slonczewski, Journal of Magnetism and Magnetic Materials **159**, L1 (1996).
6. I. M. Miron, T. Moore, H. Szambolics, L. D. Buda-Prejbeanu, S. Auffret, B. Rodmacq, S. Pizzini, J. Vogel, M. Bonfim, A. Schuhl, *et al.*, Nature materials **10**, 419 (2011).
7. S. Emori, U. Bauer, S.-M. Ahn, E. Martinez, and G. S. Beach, Nature materials **12**, 611 (2013).
8. D.-S. Han, S.-K. Kim, J.-Y. Lee, S. J. Hermsdoerfer, H. Schultheiss, B. Leven, and B. Hillebrands, Applied Physics Letters **94**, 112502 (2009).
9. P. Yan, X. Wang, and X. Wang, Physical review letters **107**, 177207 (2011).
10. X.-g. Wang, G.-h. Guo, Y.-z. Nie, G.-f. Zhang, and Z.-x. Li, Physical Review B **86**, 054445 (2012).
11. J.-S. Kim, M. St¨ark, M. Kla¨ui, J. Yoon, C.-Y. You, L. Lopez-Diaz, and E. Martinez, Physical Review B **85**, 174428 (2012).
12. X. Wang, P. Yan, J. Lu, and C. He, Annals of Physics **324**, 1815 (2009).
13. X. Wang, P. Yan, and J. Lu, EPL (Europhysics Letters) **86**, 67001 (2009).
14. D. Atkinson, D. A. Allwood, G. Xiong, M. D. Cooke, C. C. Faulkner, and R. P. Cowburn, Nature materials **2**, 85 (2003).
15. G. S. Beach, C. Nistor, C. Knutson, M. Tsoi, and J. L. Erskine, Nature materials **4**, 741 (2005).
16. M. Hayashi, L. Thomas, Y. B. Bazaliy, C. Rettner, R. Moriya, X. Jiang, and S. Parkin, Physical Review Letters **96**, 197207 (2006).
17. L. Berger, Physical Review B **54**, 9353 (1996).
18. S. Zhang and Z. Li, Physical review letters **93**, 127204 (2004).
19. G. Tatara and H. Kohno, Physical review letters **92**, 086601 (2004).
20. A. Yamaguchi, T. Ono, S. Nasu, K. Miyake, K. Mibu, and T. Shinjo, Physical review letters **92**, 077205 (2004).
21. A. Yamaguchi, A. Hirohata, T. Ono, and H. Miyajima, Journal of Physics: Condensed Matter **24**, 024201 (2011).

22. D. Hinzke and U. Nowak, Physical review letters **107**, 027205 (2011).
23. A. A. Kovalev and Y. Tserkovnyak, EPL (Europhysics Letters) **97**, 67002 (2012).
24. X. Wang, P. Yan, and X. Wang, IEEE transactions on magnetics **48**, 4074 (2012).
25. J.-P. Tetienne, T. Hingant, J.-V. Kim, L. H. Diez, J.-P. Adam, K. Garcia, J.-F. Roch, S. Rohart, A. Thiaville, D. Rav- elosona, *et al.*, Science **344**, 1366 (2014).
26. J. Torrejon, G. Malinowski, M. Pelloux, R. Weil, A. Thiaville, J. Curiale, D. Lacour, F. Montaigne, and M. Hehn, Physical review letters **109**, 106601 (2012).
27. A. Ramsay, P. Roy, J. Haigh, R. Otxoa, A. Irvine, T. Janda, R. Campion, B. Gallagher, and J. Wunderlich, Physical review letters **114**, 067202 (2015).
28. W. Jiang, P. Upadhyaya, Y. Fan, J. Zhao, M. Wang, L.-T. Chang, M. Lang, K. L. Wong, M. Lewis, Y.-T. Lin, *et al.*, Physical review letters **110**, 177202 (2013).
29. G. E. Bauer, E. Saitoh, and B. J. Van Wees, Nature materials **11**, 391 (2012).
30. C. Safranski, I. Barsukov, H. K. Lee, T. Schneider, A. Jara, A. Smith, H. Chang, K. Lenz, J. Lindner, Y. Tserkovnyak, *et al.*, Nature communications **8**, 1 (2017).
31. F. Schlickeiser, U. Ritzmann, D. Hinzke, and U. Nowak, Physical review letters **113**, 097201 (2014).
32. X. Wang and X. Wang, Physical Review B **90**, 014414 (2014).
33. P. Yan, Y. Cao, and J. Sinova, Physical Review B **92**, 100408 (2015).
34. S. K. Kim and Y. Tserkovnyak, Physical Review B **92**, 020410 (2015).
35. W. Wang, M. Albert, M. Beg, M.-A. Bisotti, D. Chernyshenko, D. Cort´es-Ortuño, I. Hawke, and H. Fangohr, Physical review letters **114**, 087203 (2015).
36. W. F. Brown Jr, Physical review **130**, 1677 (1963).
37. T. L. Gilbert, IEEE transactions on magnetics **40**, 3443 (2004).
38. A. Vansteenkiste, J. Leliaert, M. Dvornik, M. Helsen, F. Garcia-Sanchez, and B. Van Waeyenberge, AIP advances **4**, 07133 (2014).
39. G. Beach, C. Knutson, C. Nistor, M. Tsoi, and J. Erskine, Physical Review Letters **97**, 057203 (2006).